CUPCAKE: A COMPRESSION OPTIMIZER FOR SCALABLE COMMUNICATION-EFFICIENT DISTRIBUTED TRAINING

Zhuang Wang [1] **Xinyu Crystal Wu** [1] **Zhaozhuo Xu** [1] **T. S. Eugene Ng** [1]

ABSTRACT

Data-parallel distributed training (DDT) is the de facto way to accelerate deep learning on multiple GPUs. In DDT, communication for gradient synchronization is the major efficiency bottleneck. Many gradient compression (GC) algorithms have been proposed to address this communication bottleneck by reducing the amount of communicated data. Unfortunately, it has been observed that GC only achieves moderate performance improvement in DDT, or even harms the performance.

In this paper, we argue that the current way of deploying GC in a layer-wise fashion reduces communication time but at the cost of non-negligible compression overheads. To address this problem, we propose `Cupcake`, a compression optimizer to fully unleash GC algorithms' advantages in accelerating DDT. It applies GC algorithms in a *fusion* fashion and determines the provably optimal fusion strategy to maximize the training throughput of compression-enabled DDT jobs. Experimental evaluations show that GC algorithms with `Cupcake` can achieve up to 2.03× speedup in training throughput over training without GC, and up to 1.79× speedup over the state-of-the-art approaches of applying GC to DDT in a layer-wise fashion.

1 INTRODUCTION

Deep Neural Networks (DNN) are gaining rapid popularity in various domains, such as computer vision (He et al., 2016; Szegedy et al., 2016; Simonyan & Zisserman, 2014) and natural language processing (NLP) (Devlin et al., 2018; Kiros et al., 2015; Manning et al., 2014). Because DNN models introduce million-scale weight tensors, large batch training over these giant tensors is infeasible due to the limited GPU memory resources.

To overcome this obstacle, data-parallel distributed training (DDT) has been widely adopted to accelerate the training of DNN models. DDT uses multiple GPUs and each GPU has a replica of the training model (Li et al., 2014). The training dataset is partitioned into multiple parts and each GPU only trains on its partition. DDT scales DNN training over a large number of GPUs to reduce the total training time (Sergeev & Del Balso, 2018; ByteDance, 2020; Li et al., 2020).

However, there exists an exacerbating tension between computation and communication in DDT. The computation time of DNN training has been dramatically reduced thanks to the recent advancements in GPU architectures (Luo et al., 2018; NVIDIA, 2021) and domain-specific compiler techniques (Chen et al., 2018; Zheng et al., 2020). This trend leads to more frequent gradient synchronization in DDT and puts higher pressure on the network connecting GPUs. However, it is difficult for the cloud network bandwidth to keep up with the pace of computation-related improvement. Moreover, the number of GPUs for DNN training keeps increasing due to the ever-growing training dataset, which further worsens the communication time (Jiang et al., 2020). Communication has become a well-known efficiency bottleneck in DDT as each GPU needs to transmit the full gradients for synchronization (Fei et al., 2021; Huang et al., 2019; Aji & Heafield, 2017; Lin et al., 2017).

Gradient compression (GC) is a promising approach to alleviate the communication bottleneck in DDT by significantly reducing the amount of communicated data. A plethora of GC algorithms (Strom, 2015; Lin et al., 2017; Tsuzuku et al., 2018; Alistarh et al., 2017; Seide et al., 2014; Aji & Heafield, 2017; Wen et al., 2017; Karimireddy et al., 2019) have been proposed recently and they can save up to 99.9% of the gradient exchange while preserving the training accuracy and convergence (Wu et al., 2018; Stich et al., 2018; Jiang & Agrawal, 2018; Wang et al., 2022).

However, it is challenging to achieve the desired speedup when applying GC to DDT jobs (Bai et al., 2021; Agarwal et al., 2022). In this paper, we first analyze the practical difficulty of compression-enabled DDT jobs. The state-of-

[1]Computer Science Department, Rice University, Houston, TX, USA. Correspondence to: T. S. Eugene Ng <eugeneng@cs.rice.edu>.

Proceedings of the 6^{th} MLSys Conference, Miami, Florida, USA, 2023.

the-art approach for applying GC to DDT is in a *layer-wise* fashion, i.e., tensors are compressed one by one when they are ready for communication. It can greatly shorten the communication time for gradient synchronization because of the reduced amount of traffic volume. However, we surprisingly observed that the end-to-end training speedups of DDT with the layer-wise compression are only modest, and even worse than training without GC in many cases due to the incurred prohibitive overhead of compression operations (Xu et al., 2020; Wang et al., 2022).

We then propose `Cupcake` to maximize the training throughput of compression-enabled DDT by reducing the amount of communicated data and minimizing the compression overhead simultaneously. `Cupcake` is a general compression optimizer to enable GC algorithms to unleash their benefits to accelerate DDT. Essentially, GC reduces the communication time of DDT at the cost of the compression overheads. Because of the fixed overheads to launch and execute kernels in CUDA (Arafa et al., 2019), the compression overhead is non-negligible even for a small tensor size. Fortunately, we observe that this overhead keeps constant when the tensor size is smaller than a threshold (e.g., 4 MB in our testbed) and it then linearly increases with the tensor size. This observation motivates us to fuse multiple tensors for one compression operation.

Fusing tensors for compression leads to a trade-off between the reduced compression overhead and the communication overhead, i.e., the communication time that cannot overlap with computation. Because communication overlaps with computation in DDT (Zhang et al., 2017; Sergeev & Del Balso, 2018; ByteDance, 2020; Li et al., 2020), gradient tensors can begin their communications whenever they are ready in the layer-wise fashion. However, in a fusion fashion, a tensor has to wait for its following tensors for a unified compression operation and communication operation. Therefore, fusion can delay communications, shrink the overlapping time, and thus worsen the iteration time. To address this challenge, `Cupcake` determines the provably optimal fusion strategy for applying GC to DDT by balancing the compression overhead and the communication overhead. It can maximize the training throughput of compression-enabled DDT jobs, regardless of different training models, GC algorithms, and training system configurations, such as the number of GPUs and network bandwidth.

Our evaluations in both computer vision and NLP demonstrate that GC algorithms applied with `Cupcake` can greatly improve the training throughput of DDT. Specifically, `Cupcake` enables GC algorithms to achieve up to $2.03\times$ speedup in training throughput over training without GC, and up to $1.79\times$ speedup over the state-of-the-start solutions that compress tensors in a layer-wise fashion.

2 Background

2.1 Data-parallel Distributed Training

Data-intensive training of DNNs on powerful Graphic Processing Units (GPU) (Owens et al., 2008) boosts the success of deep learning (LeCun et al., 2015). Given the massive amount of training dataset, data-parallel distributed training (DDT) (Shallue et al., 2019; Ben-Nun & Hoefler, 2019; Li et al., 2020) has become one of the most popular paradigms to scale out deep learning with multiple GPUs. In this paradigm, the training dataset is partitioned into multiple subsets. Each GPU has a replica of the training model that trains on a specific subset. In each iteration, each GPU consumes a mini-batch from its allocated subset as the input of the training. Next, it propagates the mini-batch through the neural network model and calculates the loss function via *forward propagation*. Then, it uses the loss value to compute the gradients of each parameter in *backpropagation*. Finally, it *synchronizes* the gradient updates from all GPUs to update the model parameters with a certain optimizer, such as SGD (Zinkevich et al., 2010) or Adam (Kingma & Ba, 2014). Training a DNN model is a process to refine the model parameters with the above steps iteratively until its convergence. Asynchronous DDT, where GPUs do not wait for the synchronized results to begin the next iteration, can hurt the model accuracy (Chen et al., 2016). In this paper, we focus on synchronous DDT because of its wide adoption (ten, 2016; ByteDance, 2020; Sergeev & Del Balso, 2018; Li et al., 2020).

2.2 Communication Bottleneck in DDT

The single-GPU iteration time of DNN training jobs has been significantly reduced thanks to the advancement of DNN accelerators and domain-specific compiler techniques. For example, the iteration time of ResNet50 with one GPU has decreased by $22\times$ in the last six years (Sun et al., 2019). However, network upgrades have not kept up with the pace of computation-related advancements. The cloud network bandwidth has only witnessed a roughly $10\times$ increase in the same period (Mellanox, 2022). This imbalance between the fast-growing computing capability and the slower-growing communication bandwidth worsens the communication-computation tense in DDT (Wang et al., 2023).

Single precision (FP32) is a common floating point format representing the weights and gradients in deep learning. When gradients are communicated in FP32 for synchronization, it can lead to costly communication time and thus poor scalability in DDT. It has been reported that the communication time for gradient synchronization accounts for over 60% of the total time for the training of BERT (Devlin et al., 2018) or other Transformer models across 16 AWS EC2 instances, each with 8 NVIDIA V100 GPUs, in a 100Gbps network (Bai et al., 2021; Wang et al., 2023).

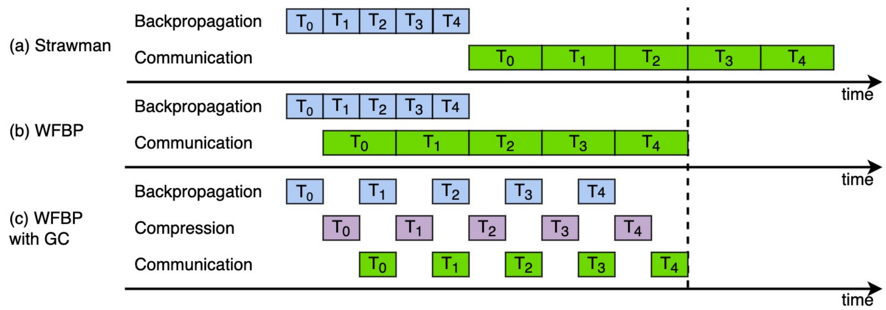

Figure 1. An example of DDT with five tensors for gradient synchronization. (a) is the strawman in which communications have to wait for the completion of backpropagation. (b) uses WFBP to overlap communication with backpropagation to reduce the iteration time. In (c), every tensor is compressed, but it does not reduce the iteration time compared to (b) due to the compression overheads. Forward propagation and decoding are omitted.

When the network bandwidth in GPU clouds cannot keep pace with the improvements in computation, an alternative is to shrink the communicated data volume by applying gradient compression to DDT.

2.3 Gradient Compression Algorithms

Many gradient compression (GC) algorithms have been proposed recently to reduce the amount of communicated data volume for gradient synchronization. There are two main types of GC algorithms: *Sparsification* and *Quantization*. Sparsification selects a subset of the original stochastic gradients for synchronization (Wang et al., 2022; Aji & Heafield, 2017; Lin et al., 2017) and it can save up to 99.9% of the gradient exchange (Lin et al., 2017). Quantization decreases the precision of gradients. The gradients in FP32 are mapped to fewer bits, such as 8 bits (Dettmers, 2015), 2 bits (Wen et al., 2017), and even 1 bit (Seide et al., 2014; Karimireddy et al., 2019; Bernstein et al., 2018) to reduce the communicated traffic volume by up to 96.9%. Such compression algorithms have been theoretically proved and/or empirically validated to preserve the convergence of model training and impose negligible impact on model accuracy when combined with error-feedback mechanisms (Seide et al., 2014; Wu et al., 2018; Stich et al., 2018; Lin et al., 2017; Jiang & Agrawal, 2018). There are also other types of GC algorithms, such as low-rank decomposition (Vogels et al., 2019; Wang et al., 2018a) and FFT-based compression (Wang et al., 2020).

2.4 Overlapping Communication with Computation

Because of the layered structure and a layer-by-layer computation pattern in DNN models, the wait-free backpropagation mechanism (WFBP) (Zhang et al., 2017; Sergeev & Del Balso, 2018; ByteDance, 2020; Li et al., 2020; Chen et al., 2015) is widely adopted to overlap communication with computation in DDT. As illustrated in Figures 1(a) and 1(b), WFBP can significantly reduce the iteration time compared to the strawman solution, in which communication cannot begin until the completion of backpropagation. Existing distributed ML frameworks, such as PyTorch (Paszke et al., 2019), Tensorflow (ten, 2016), and Horovod (Sergeev & Del Balso, 2018), apply GC to DDT in a *layer-wise fashion*, i.e., tensor by tensor, to overlap communication with computation because of WFBP.

3 The Practical Performance of GC with Layer-wise Compression

Because applying GC to DDT requires computation resources, it competes for GPU resources with backpropagation and delays tensor computation, as shown in Figure 1(c). Although GC algorithms can reduce the communication time of DDT, the incurred compression overheads can dramatically dilute the benefits gained from the reduced communication time.

To demonstrate, we empirically measure the training speeds of compression-enabled DDT with several popular GC algorithms, including both sparsification and quantization. The experiments are conducted on a server equipped with 8 GPUs (NVIDIA Tesla V100 with 32 GB memory), two 20-core/40-thread processors (Intel Xeon Gold 6230 2.1GHz), and PCIe 3.0×16. We use GRACE (Xu et al., 2020) as the framework to support compression-enabled DDT and GC algorithms are applied in a layer-wise fashion. The training model is ResNet50 (He et al., 2016) over CIFAR10 (Krizhevsky et al., 2009) and the batch size is 32.

Two sparsification algorithms, DGC (Lin et al., 2017) and Rand-k (Stich et al., 2018), are evaluated and the gradient sparsity is 99%, i.e., only 1% of gradients are exchanged during synchronization. Two 1-bit quantization algorithms,

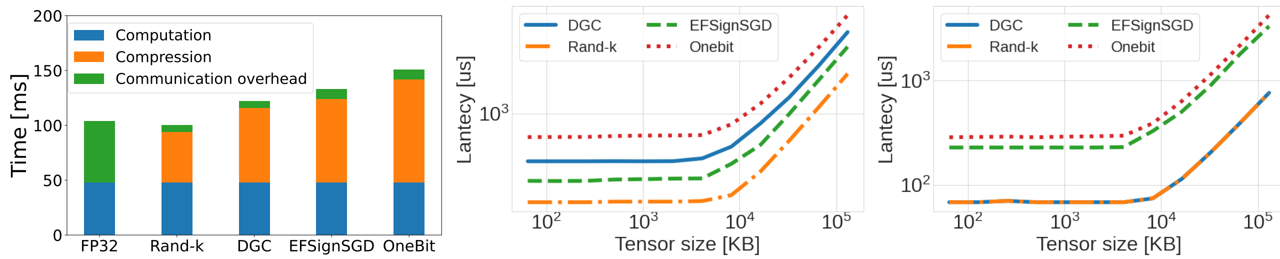

(a) Time breakdown of one iteration (b) Encoding overhead (c) Decoding overhead

Figure 2. The compression overheads with different compression algorithms. The data in (a) are collected from the training of ResNet50; the data in (b) and (c) are collected from a microbenchmark. Both encoding and decoding overheads are non-negligible.

EFSignSGD (Karimireddy et al., 2019) and OneBit (Seide et al., 2014) are also evaluated.

Figure 2a shows the breakdown of the iteration time of the training. The *communication overhead* refers to the communication time that cannot overlap with backpropagation and compression of any tensors. FP32 is the training baseline without GC. We observe that the performance improvement with these GC algorithms is modest. Some algorithms, such as DGC, EFSignSGD, and OneBit, even surprisingly lead to a longer iteration time. This observation is on par with the findings in prior works (Xu et al., 2020; Sapio et al., 2019; Li et al., 2018; Gupta et al., 2020; Agarwal et al., 2022).

3.1 The Root Cause of the Poor Performance

When a gradient tensor is ready for synchronization in DDT without compression, it is communicated and then the aggregated results are used to update the training model. However, there are two additional operations when applying GC to DDT: encoding (encode a tensor before communication to reduce the traffic volume) and decoding (decode the received compressed tensor for model updates) [1] These two operations can incur non-negligible computation overhead.

Figure 2b and 2c display the encoding and decoding latencies with four representative GC algorithms, i.e., DGC (Lin et al., 2017) and Rand-k (Stich et al., 2018) for sparsification, EFSignSGD (Karimireddy et al., 2019) and Onebit (Seide et al., 2014) for quantization. Both encoding and decoding latencies are non-negligible, even for tensors with small sizes. For instance, the encoding latencies of DGC, EFSignSGD, and Onebit are all greater than 0.25 ms, regardless of the tensor sizes.

DNN models typically have a large number of tensors for gradient synchronization (He et al., 2016; Devlin et al., 2018). The layer-wise compression invokes encoding and decoding operations for each tensor and leads to prohibitive compression overheads. We take training ResNet50 over CIFAR10 with 8 GPUs in our testbed as a concrete example to compare the overall compression overhead against the communication improvement. In our measurement, the iteration time of the single-GPU training is around 48 ms. Without any compression, the communication overhead in each iteration is about 56 ms. Both sparsification and 1-bit quantization algorithms can reduce the communication overhead to less than 10 ms thanks to the much smaller communicated traffic volume. However, the overall compression overheads of DGC and EFSignSGD are both larger than 60 ms, which is even higher than the communication overhead in the baseline. The costly compression overheads result in the poor practical performance of DDT with GC.

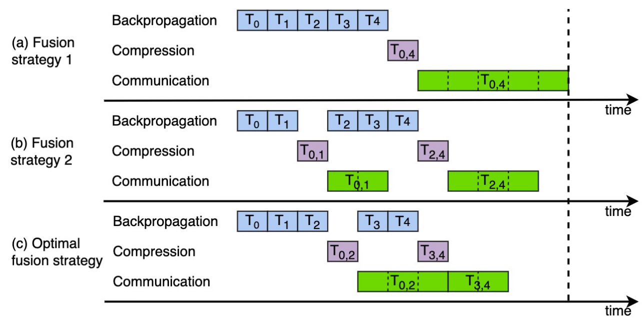

Figure 3. `Cupcake` fuses multiple tensors for one compression operation and one communication operation to minimize the iteration time. It is challenging to find the optimal fusion strategy given a DDT job and a GC algorithm because fusing tensors leads to a trade-off between the reduced compression overhead and the overlapping time between communication and backpropagation.

3.2 An Opportunity and a Challenge

The compression overhead of GC algorithms with a layer-wise fashion becomes the new efficiency bottleneck in DDT. We observe that there are some fixed overheads to launch and execute kernels in CUDA (Arafa et al., 2019). Figure 2 shows that the encoding and decoding latencies of GC al-

[1] It may require more decoding operations after communication when multiple encoded tensors are received on each GPU.

gorithms keep constant when the tensor size is smaller than a threshold (e.g., 4 MB in our testbed). They then almost linearly increase with the tensor sizes. This observation indicates that fusing multiple tensors for one compression operation can potentially reduce the overall compression overhead and thus the iteration time. Suppose there are ten tensors with a size of 128 KB for gradient synchronization and the encoding latency of DGC for a 128 KB tensor is 0.4 ms. If we can fuse these ten tensors for one encoding operation, the overall encoding latency is still 0.4 ms, which is significantly lower than the latency incurred by ten encoding operations for the ten tensors separately.

However, fusing tensors for GC algorithms raises a new challenge: what is the optimal fusion strategy to minimize the iteration time? There is a trade-off between the compression overhead and the communication overhead because fusing tensors to reduce the compression overhead has to delay communications and thus shrink the overlapping time between communication and computation (including both backpropagation and compression). For example, an extreme case of tensor fusion is applying a GC algorithm to an entire training model with only one compression operation. However, in this case, communication cannot begin until the completion of backpropagation, resulting in suboptimal communication overhead, as shown in Figure 3(a). Another extreme case is to apply the layer-wise fashion to compress tensors one by one to minimize the communication overhead, but it leads to prohibitive compression overheads, as discussed in Section 3.1.

There are numerous fusion strategies to apply a GC algorithm to a DDT job and three strategies are illustrated in Figure 3. It is challenging to find the optimal one because it depends on many factors, such as the applied GC algorithms, the tensor size and the computation time of the DNN model, the number of GPUs, and network bandwidth. We must jointly consider backpropagation, compression, and communication overheads to search for the optimal strategy to maximize the training throughput of compression-enabled DDT jobs.

4 CUPCAKE

In this section, we first formulate the tensor fusion problem given a DDT job and a GC algorithm. We then design an algorithm to provably find the optimal fusion strategy to minimize the iteration time.

4.1 Problem Formulation

The core idea of Cupcake is to fuse multiple tensors for one compression operation, instead of applying GC to DDT in a layer-wise fashion. It can reduce the compression overhead and meanwhile overlap communication with computation to reduce the communication overhead.

Given a training model with N tensors, the set of tensors is $\mathcal{T} = \{T_0, \dots, T_{N-1}\}$. For example, Figure 1 and Figure 3 display a training model with five tenors. Cupcake partitions the model into y groups and determines a fusion strategy $\mathcal{X}_y = \{\mathrm{x}_0, \dots, \mathrm{x}_{\mathrm{y}-1}\}$, where x_i is a group of consecutive tensors that are compressed and communicated together. Cupcake performs an encoding operation and a communication operation for each tensor group in each iteration. After encoding, the fused tensor x_i is communicated and synchronized. After communication, the encoded x_i is decoded and aggregated to update the training model.

Let A denote the computation time for forward propagation in an iteration and $B(T_i)$ denote the computation time of T_i in backpropagation. x_i is the total tensor size of x_i. $h(\mathrm{x}_i)$ is the time to compress x_i and $g(\mathrm{x}_i)$ is the corresponding communication time. $P(\mathcal{X}_y)$ is the total overlapping time, i.e., the total communication time that overlaps with the compression and backpropagation of any tensors. Given a fusion strategy $\mathcal{X}_y = \{\mathrm{x}_0, \dots, \mathrm{x}_{y-1}\}$, the iteration time is

$$f(\mathcal{X}_y) = A + \sum_{b=0}^{N-1} B(T_i) + \sum_{i=0}^{y-1} h(\mathrm{x}_i) + \sum_{i=0}^{y-1} g(\mathrm{x}_i) - P(\mathcal{X}_y). \quad (1)$$

A and $B(T_i)$ can be profiled offline for a training model and they are constant across iterations (Zhang et al., 2020; Sun et al., 2019). Following the literature (Thakur et al., 2005; NCC, 2021; Fei et al., 2021; Renggli et al., 2019), we model the communication time of x_i as $g(\mathrm{x}_i) = \alpha_g + \beta_g x_i$, where α_g is the latency (or startup time) per tensor and β_g is the transfer time per byte after encoding. Based on the measurement in Figure 2, we model the compression time of x_i as $h(\mathrm{x}_i) = \alpha_h + \beta_h x_i$, where α_h is the fixed overhead to launch and execute kernels in CUDA and β_g is the compression time per byte. Cupcake measures α_g, β_g, α_h, and β_h offline based on the system configurations, such as the GPU computation capacity, the number of GPUs, and the network bandwidth.

Given a fusion strategy, Cupcake can calculate its iteration time by deriving the timelines of its backpropagation, compression, and communication (Wang et al., 2023), as shown in Figure 3. Unfortunately, it is still challenging to formulate $f(\mathcal{X}_y)$ due to $P(\mathcal{X}_y)$, which is determined by the strategy and the intricate interactions among backpropagation, compression, and communications of all the tensors.

Instead of deriving the expression of $P(\mathcal{X}_y)$, we formulate the tensor fusion problem in a recursive way to minimize the iteration time of a DDT job with a given GC algorithm. Let $F(M, i)$ be the iteration time of the optimal fusion strategy from T_i to T_{N-1}, given the fusion strategy for tensors from T_0 to T_{i-1} is represented by M. We then have the following recurrence relation

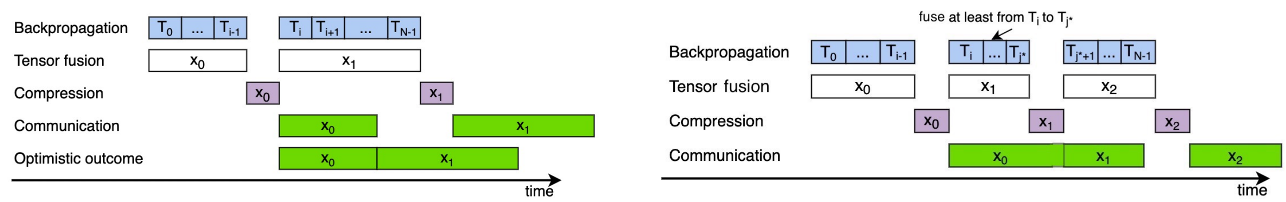

(a) Cupcake prunes a strategy if its optimistic outcome is greater than the current optimal iteration time when determining x_0.

(b) Cupcake prunes strategies in which x_1 fuses tensors from T_i to T_j, where $j < j^*$, when x_0 is determined.

Figure 4. Examples of the two pruning techniques.

$$\begin{cases} F(\{\}, 0) = \min\limits_{1 \le i \le N} F(\{\text{fuse}(0, i-1)\}, i), & (2) \\ F(M, i) = \min\limits_{i+1 \le j \le N} F(M + \text{fuse}(i, j-1), j), & (3) \end{cases}$$

where fuse(i, j) fuses tensors from T_i to T_j as one group. Cupcake first considers the form of x_0, i.e., fuse$(0, i-1)$, where $1 \le i \le N$, in Equation (2). It then recursively computes $F(M, i)$ to find the optimal fusion strategy for the entire model. For simplicity, let $h(i, j)$ denote the compression time of a fused tensor from T_i to T_j, $g(i, j)$ denote its communication time, and $B(i, j)$ denote its backpropagation time.

4.2 The Optimal Fusion Strategy

For any tensor in a DNN model except T_0, it can be either fused into the current group or form a new one. Therefore, there are 2^{N-1} possible fusion strategies. It indicates that the time complexity to address the tensor fusion problem with brute force is exponential. Because DNN models typically have hundreds of tensors, it is impractical to enumerate all possible strategies. Moreover, the optimal strategy is specific to each situation because different DDT jobs have different characteristics, such as different tensor numbers, different tensor sizes, and different system configurations.

We first introduce two pruning techniques based on two insights to enable Cupcake to find the optimal fusion strategy efficiently.

Insight #1: It is not necessary for Cupcake to examine all the N cases for the formation of x_0. When there are too many tensors in x_0, it can delay communication and lead to a long iteration time. Given a case of x_0, we can calculate the *optimistic outcome* of the iteration time as follows.

$$\begin{aligned} &F(\{\text{fuse}(0, i-1)\}, i) \ge \\ &\max\{B(0, N-1) + h(0, i-1) + h(i, N-1), \\ &\quad B(0, i-1) + h(0, i-1) + g(0, i-1) + g(i, N-1)\}. \end{aligned} \tag{4}$$

The optimistic outcome considers two cases. The first case is that there is no communication overhead. The second case is that except tensors in x_0, all the other tensors are fused as one group for compression and communication, and x_1's communication begins right after x_0's communication, as shown in Figure 4a. The compression time of x_1 is perfectly overlapped with communication. If the optimistic outcome of a case is already greater than the iteration time of the best fusion strategy found so far, then this case, i.e., the recursive computation for $F(\{\text{fuse}(0, i-1)\}, i)$, can be pruned.

Insight #2: It is safe to fuse more tensors in a group based on the progress of communication of the previous group. Suppose x_0 is fused from T_0 to T_{i-1}. We apply Equation (3) recursively to enumerate cases for x_1, which fuses tensors from T_i to T_j. The backpropagation time and the compression time of x_1 can overlap with x_0's communication, as shown in Figure 4b. The smallest j can be calculated with

$$j^* = \arg\max_j \{B(i, j) + h(i, j) \le g(0, i-1)\}. \tag{5}$$

Note that the less number of tensors in x_1 means more tensors in x_2 and DDT has to communicate more tensors after the completion of backpropagation. Fusing from T_i to T_j, where $j < j^*$, is no better than fusing from T_i to T_{j^*} because it shrinks the overlapping time between communication and computation. Therefore, Cupcake can prune the strategies in which x_1 fuses tensors from T_i to T_j where $j < j^*$ and only examine $j \ge j^*$.

Fusion Algorithm. Based on the two insights of examining possible fusion strategies, we design Algorithm 1 to find the optimal fusion strategy given a DDT job and a GC algorithm. The function `Main()` checks the N cases of x_0 and it invokes `FindOptFusion()` to recursively search for the optimal strategy (lines 1-5). `FindOptFusion()` takes two inputs M and k: $M = \{x_0, \ldots, x_{a-1}\}$, which is the fusion strategy for tensors from T_0 to T_{k-1}, and T_k is the first tensor to be fused for x_a.

Algorithm 1 uses $global\_opt\_fuse$ to store the best fusion strategy found so far and $local\_opt\_fuse$ to store the local best strategy from T_k to T_{N-1}. Given M, it first applies

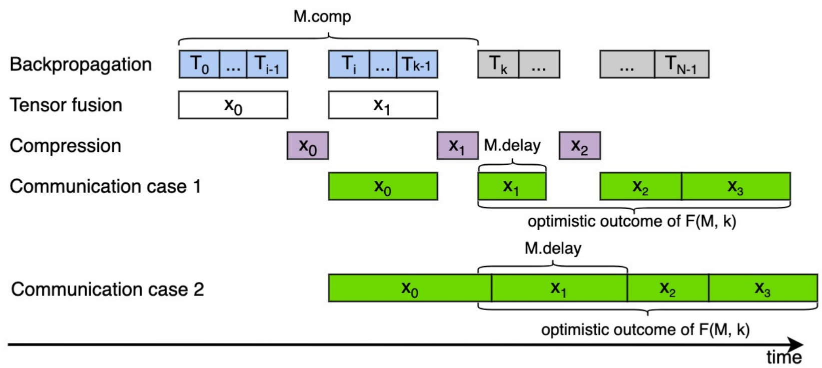

Figure 5. A general case for the two pruning techniques given M, which is the set of fused tensors from T_0 to T_{k-1}. $M.comp$ and $M.delay$ can be derived based on the timelines of backpropagation, compression, and communication of tensors in M.

the second insight to fuse the first group beginning from T_k (Lines 9-16). The example illustrated in Figure 4b only considers the case that x_{a-1}'s communication begins right after its compression, but it is likely that its communication can be delayed by communication of its previous group. The algorithm replaces $g(0, i-1)$ in Expression (5) with $M.delay$, which denotes the difference between the completion time of compression and communication of x_{a-1}. The two cases of $M.delay$ are illustrated in Figure 5. We also denote $M.comp$ as the time duration from the beginning of backpropagation to the completion of x_{a-1}'s compression, as shown in Figure 5. Given M, both $M.delay$ and $M.comp$ can be calculated based on the timelines of backpropagation, compression, and communication, regardless of the strategy to fuse the remaining tensors.

Algorithm 1 finds j^* based on $M.delay$ (Lines 9-16) to skip the enumerations of tensors from T_k to T_{j^*-1}. It then uses the first insight to calculate the optimistic outcome (Lines 19-21). Similarly, the example shown in Figure 4a only considers the case that x_a's communication begins right after its compression. However, it is also likely that its communication can be delayed by x_{a-1}'s communication, as shown in Communication case 2 in Figure 5. The algorithm considers both cases and calculates the optimistic outcome. Algorithm 1 prunes the search if the optimistic outcome is already greater than the iteration time of the current best strategy. Suppose x_a is fused from T_k to T_i, `FindOptFusion()` recursively applies itself to find the local optimal fusion strategy from T_{i+1} to T_{N-1} (Lines 25-28). It updates $local\_opt\_fuse$ and $global\_opt\_fuse$ if the current strategy is better (Lines 29-36).

In practice, Algorithm 1 can use a heuristic to bootstrap $global\_opt\_fuse$ with a relatively good fusion strategy. For example, it can partition a DNN model into multiple groups (e.g., two groups) with the same number of tensors.

Time complexity. The complexity of Algorithm 1 is $O(2^N)$ because it has to enumerate all fusion strategies in the worst case. Fortunately, the two pruning techniques can prune most of them and enable `Cupcake` to find the optimal one quickly, as we will show in Section 5.3.

Theorem 1. *Algorithm 1 finds the optimal fusion strategy that minimizes the iteration time of a DDT job given a GC algorithm.*

Proof. Algorithm 1 recursively invokes function `FindOptFusion`(M, k). Let $n = N - k$, which is the number of tensors this function considers. We use induction on n to prove that the function finds the optimal fusion strategy from T_k to T_{N-1} given M.

Base case. When $n = 1$, the function only needs to examine one tensor and thus only one fusion strategy, which is the optimal one.

Inductive step. Assume that for any $1 \leq n \leq p$, `FindOptFusion`(M, k) returns the optimal fusion strategy from T_k to T_{N-1} given M. Consider $n = p + 1$. Algorithm 1 divides the problem into $p + 1$ cases, where case i ($0 \leq i \leq p$) fuses the first group from T_k to T_{k+i}.

We first consider case i where $0 \leq i \leq p - 1$. The function invokes `FindOptFusion`$(M+fuse(k, k+i), k+i+1)$, in which the number of tensors considered is $p - i \leq p$. Hence, it outputs the optimal strategy for case i based on the assumption. We then consider case $i = p$ and the first group is fused from T_k to T_{N-1}. This is the only fusion strategy and thus the optimal one. Because these cases are exclusive and cover the entire search space, Algorithm 1 finds the optimal fusion strategy for $n = p+1$ by searching for the optimal one from these cases.

Algorithm 1 applies two pruning techniques to quickly find the optimal fusion strategy. The first one prunes the cases whose lower bounds are no better than the optimal found so far and it has no impact on the optimality. The second one prunes the cases whose first groups are fused from T_k to T_j,

Algorithm 1: Optimal Fusion Strategy

Input: N is the number of tensors in a DNN model.
$global\_opt\_fuse = \{\}$. $global\_opt\_time = \infty$
Output: The optimal fusion strategy $global\_opt\_fuse$.

Function `Main()`**:**
  for $k \leftarrow 1$ **to** N **do**
    `FindOptFusion`({fuse(0, k-1)}, k)
  end
  return $global\_opt\_fuse$
Function `FindOptFusion(`M, k`)`**:**
  $local\_opt\_fuse \leftarrow \{\text{fuse}(k, N-1)\}$
  `// f() is defined in Equation (1)`
  $local\_opt\_time \leftarrow f(M + \text{fuse}(k, N-1))$
  $j^* \leftarrow k$
  for $i \leftarrow k$ **to** $N-1$ **do**
    if $B(k,i) + h(k,i) \leq M.delay$ **then**
      $j^* \leftarrow i$
    else
      break
    end
  end
  $M.comp = B(0, k-1) + \sum_{x \in M} h(x)$
  for $i \leftarrow j^*$ **to** $N-1$ **do**
    $base \leftarrow B(k, N-1) + h(k,i) + h(i+1, N-1)$
    $cases \leftarrow \max\{B(k,i) + h(k,i), M.delay\} + g(k,i) + g(i+1, N-1)$
    $optim\_outcome \leftarrow M.comp + \max(base, cases)$
    if $optim\_outcome > global\_opt\_time$ **then**
      continue
    end
    $first\_fuse \leftarrow \text{fuse}(k, i)$
    $rest\_fuse \leftarrow$ `FindOptFusion`$(M + first\_fuse, i+1)$
    $cur\_fuse \leftarrow first\_fuse + rest\_fuse$
    $cur\_fuse\_time = f(M + cur\_fuse)$
    if $cur\_fuse\_time < local\_opt\_fuse\_time$ **then**
      $local\_opt\_fuse \leftarrow cur\_fuse$
      $local\_opt\_time \leftarrow cur\_fuse\_time$
    end
    if $cur\_fuse\_time < global\_opt\_time$ **then**
      $global\_opt\_fuse \leftarrow M + cur\_fuse$
      $global\_opt\_time \leftarrow cur\_fuse\_time$
    end
  end
  return $local\_opt\_fuse$

where $j < j^*$. Because they cannot advance communication to an earlier point than fusing from T_k to T_{j^*}, pruning these cases does not affect the optimality. □

5 Experiments

In this section, we will first show the performance improvement of Cupcake for GC algorithms with sparsification and quantization. We then evaluate Time-to-Accuracy to demonstrate that Cupcake can preserve the accuracy of these applied GC algorithms. At last, we show that Cupcake can find the optimal fusion strategy quickly.

Setup. Two testbed setups are used for the evaluations. The first setup is the same as that described in Section 3. The server has 8 GPUs and they are connected by PCIe 3.0 $\times 16$. The second setup has 8 GPU machines connected to a 25Gbps network. Each machine has 8 NVIDIA Tesla V100 GPUs (32 GB GPU memory) connected by NVLink and 48-core/96-thread processors (Intel Xeon 8260 at 2.40GHz). The server has an Ubuntu 18.04.4 LTS system and the software environment includes PyTorch-1.8.1, Horovod-0.22.1, CUDA-11.1, and NCCL-2.9.9.

Workloads. We validate the performance of Cupcake on two types of machine learning tasks: computer vision and natural language processing (NLP). The models include ResNet50 over CIFAR10 (Krizhevsky et al., 2009) and ResNet101 (He et al., 2016) over ImageNet-1K (Deng et al., 2009); BERT-base (Devlin et al., 2018) over SQuAD (Rajpurkar et al., 2018). These models are widely used as standard benchmarks to evaluate the scalability of DDT. The batch sizes for ResNet50 and ResNet101 are 32 and for BERT-base are 1024 samples.

Compression algorithms. We use four representative GC algorithms: Rand-k (Stich et al., 2018) and DGC (Lin et al., 2017) for sparsification with 99% sparsity, and EF-SignSGD (Karimireddy et al., 2019) and OneBit (Seide et al., 2014) for quantization. Error-feedback (Karimireddy et al., 2019; Lin et al., 2017) is applied to GC algorithms to preserve the model accuracy.

Baselines. We use Horovod (Sergeev & Del Balso, 2018) as the training baseline without GC (FP32). We use GRACE (Xu et al., 2020) and HiPress (Bai et al., 2021) as the two layer-wise baselines for applying GC to DDT. GRACE applies GC to all tensors in a model and HiPress only compresses tensors greater than a threshold, which is determined by the tensor size, network bandwidth, and compression overhead.

Metrics. Suppose the training speed with n GPUs is T_n. The scaling factor (Zhang et al., 2020) is defined as $\frac{T_n}{nT_1}$. We use the scaling factor, Top-1 accuracy, and F1 score as evaluation metrics. The results for scaling factors are reported with an average of 100 iterations. We also report the standard deviation using the error bar because the training speed varies at times.

Allgather for communications. Allreduce is used for communications in FP32 (Sergeev & Del Balso, 2018; Paszke et al., 2019). Existing frameworks' implementation of Allreduce requires tensors to be aligned and support element-wise aggregations. However, compressed tensors typically do not satisfy these requirements. For example, compressed tensors using Rand-k have different indices for selected elements, while those using Onebit cannot support addition. In contrast, the implementation of Allgather (Thakur et al., 2005) has no such restrictions. It gathers tensors from all

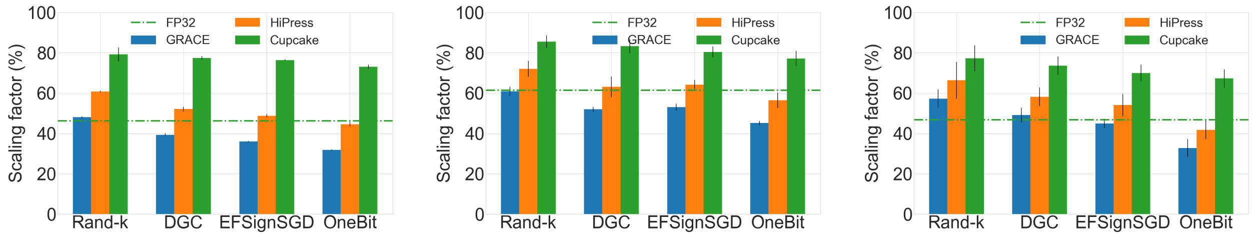

(a) ResNet50 (b) ResNet101 (c) BERT-base

Figure 6. The scaling factors of three DNN models running on a server with 8 GPUs connected by PCIe 3.0 $\times 16$.

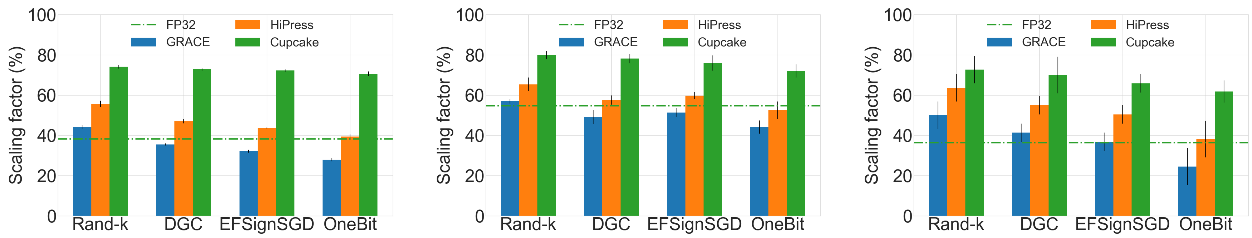

(a) ResNet50 (b) ResNet101 (c) BERT-base

Figure 7. The scaling factors of three DNN models running on 64 GPUs in 8 servers connected by a 25Gbps network.

GPUs and allows for customized aggregation operations for compressed tensors. Therefore, we chose to use Allgather in our implementation to communicate compressed tensors (Xu et al., 2020; Wang et al., 2023).

5.1 Training Speed Improvement

Figure 6 shows the scaling factors of the three DNN models running on a server with 8 GPUs connected by PCIe 3.0 $\times 16$. The four compression algorithms are applied with `Cupcake` and the two layer-wise baselines, respectively.

We can see from Figure 6 that applying GC in a layer-wise fashion can even harm the performance of DDT due to the costly compression overhead. The scaling factors of both ResNet50 and ResNet101 with GRACE compression are lower than those without any compression in most cases. HiPress outperforms GRACE because it avoids encoding small tensors and incurs less compression overhead. However, its improvement in the training throughput is just modest compared to training without GC. Applying Rand-k, DGC, and EFSignSGD to the training of BERT with HiPress can improve the training speed, but it still harms the training performance when the GC algorithm is OneBit.

In contrast, `Cupcake` significantly improves the training speed of DDT with GC algorithms for the three DNN models compared to FP32. For the training of ResNet50, it outperforms FP32 by up to 72% (apply Rand-k). It also outperforms GRACE and HiPress by up to 130% and 64% (apply OneBit), respectively. For ResNet101, `Cupcake` outperforms FP32, GRACE, and HiPress by up to 39%, 70%, and 37%, respectively. For BERT-base, it outperforms FP32, GRACE, and HiPress by up to 65%, 106%, and 61%, respectively.

Figure 7 shows the scaling factors of the three DNN models running on 8 servers (each has 8 GPUs) connected by a 25Gbps network. Because intra-machine communications are supported by NVLink, which can provide every GPU in total 1.2Tbps GPU-GPU bandwidth (Jiang et al., 2020), the performance bottleneck is inter-machine communications. Therefore, tensors are not compressed for intra-machine communications and GC is applied for inter-machine communications only. Figure 7 shows that the speedups of `Cupcake` over FP32 are up to 93%, 46%, and 103% for the training of ResNet50, ResNet101, and BERT-base, respectively. It also outperforms HiPress by up to 79%, 37%, and 58% for the training of the three models, respectively.

5.2 Time-to-Accuracy Improvement

Because HiPress is always better than GRACE in terms of the training throughput, we compare `Cupcake` to HiPress in this section. We train ResNet50 over CIFAR10 until convergence on a server with 8 GPUs connected by PCIe 3.0 $\times 16$. The applied GC algorithm is DGC. As shown in Figures 8a, `Cupcake` can achieve around 1.68$\times$ speedup over no compression (i.e. FP32), and 1.30$\times$ speedup over HiPress. The achieved Top-1 accuracy with `Cupcake` is

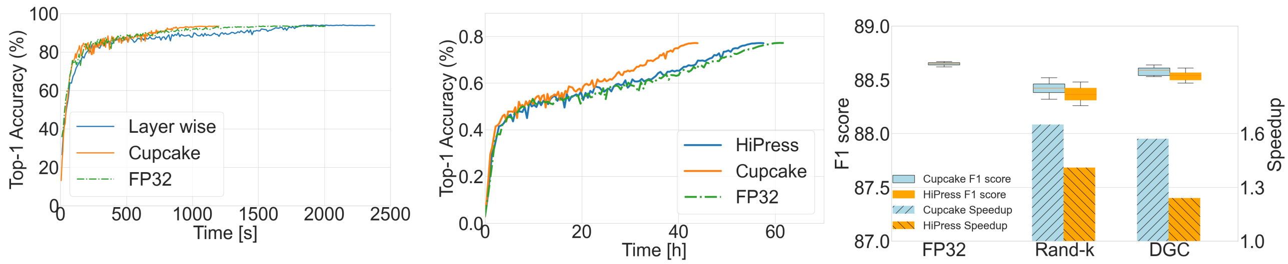

(a) ResNet50 (b) ResNet101 (c) BERT-base

Figure 8. `Cupcake` achieves almost the same model accuracy as no compression. DGC and EFSignSGD are applied to the training of ResNet50 over CIFAR10 and ResNet101 over Imagenet-1K, respectively. Both Rand-k and DGC are applied to the training of BERT-base over SQuAD.

Table 1. Running time of Algorithm 1.

	ResNet50	ResNet101	BERT-base
# of tensors	161	314	207
Algorithm 1	2.8 s	6.6 s	4.2 s
Only Pruning 1	15 s	68 s	32 s
Only Pruning 2	2.2 h	9.4 h	> 24 h
No Pruning	> 24 h	> 24 h	> 24 h

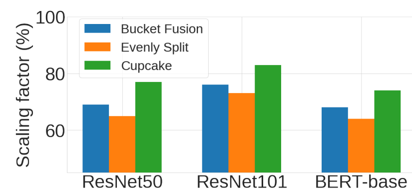

Figure 9. The scaling factors of three DNN models running on a server with 8 GPUs. The GC algorithm is DGC.

93.2% (with HiPress is 93.1%), which is very close to the no-compression accuracy of 93.6%. We also train ResNet101 for 120 epochs on ImageNet-1K from scratch and apply EFSignSGD to the model training. Figure 8b shows that `Cupcake` outperforms no compression and HiPress by 1.32× and 1.25×, respectively. The achieved Top-1 accuracy with `Cupcake`, HiPress, and no compression is 76.7%, 76.6%, and 77.1%, respectively. In addition, we conduct a test following the methodology in (Fei et al., 2021) to fine-tune BERT-base for the question-answering task on SQuAD (Rajpurkar et al., 2018) for two epochs and repeat the experiments ten times. Figure 8c shows that `Cupcake` with DGC can achieve around 1.65× speedup over no compression and it has almost the same F1 score as no compression.

5.3 Effectiveness of `Cupcake`

Computation time. We first measure the computation time of Algorithm 1 with the two pruning techniques. Note that the number of tensors in a DNN model, their sizes, and the computation time of backpropagation are measured in advance. The cost model of the communication time is determined by the network bandwidth. We also profile the encoding and decoding overheads of a GC algorithm, as shown in Figure 2, to model the compression time.

Table 1 shows that it only takes several seconds for Algorithm 1 to find the optimal fusion strategy for the three DNN models when training them on a server with 8 GPUs connected by PCIe 3.0 ×16. For example, the computation time is only a few seconds even for ResNet101 which has 314 tensors. However, the search cannot finish after running for 24 hours without the two pruning techniques, i.e., searching for the optimal strategy with brute force.

Compared to strawman solutions. We also compare `Cupcake` with the following two strawman solutions for tensor fusion.

- Bucket Fusion (Li et al., 2020; Sergeev & Del Balso, 2018). It stores tensors in a buffer and fuses tensors in the buffer when their total size exceeds a threshold. We set different thresholds from 2 MB to 64 MB and use the best performance as its performance.
- Evenly Split. It evenly splits consecutive tensors into multiple groups for fusion and each group has the same number of tensors. We set the number of groups from 2 to 32 and use the best performance as its performance.

We apply DGC with three fusion strategies, `Cupcake`, Bucket Fusion, and Evenly Split, to three DNN models when training them on a server with 8 GPUs. Figure 9 displays their scaling factors. Both Bucket Fusion and Evenly Split outperform the layer-wise baselines thanks to the reduced compression overheads. `Cupcake` outperforms them by up to 1.12× and 1.18×, respectively. `Cupcake` searches for the optimal fusion strategy from the whole search space. We observe that the number of tensors and the size of the fused tensor vary a lot across groups in the optimal strategy for the three evaluated DNN models. However, the two strawman solutions limit the search space and constrain that each group has to have the same number of tensors or the same fused tensor size, leading to suboptimal fusion strategies.

6 Related Work

Many GC algorithms (Strom, 2015; Lin et al., 2017; Tsuzuku et al., 2018; Alistarh et al., 2017; Seide et al., 2014; Aji & Heafield, 2017; Wen et al., 2017; Karimireddy et al., 2019; Shi et al., 2021; Wang et al., 2022; 2018b) have been proposed to reduce the amount of communicated traffic volume for gradient synchronization, as discussed in Section 2.3. However, they are designed from an algorithmic perspective and have no suggestion for how to efficiently apply them to DDT. In contrast, `Cupcake` is not a GC algorithm, but a compression optimizer to maximize the benefits of GC algorithms from a system perspective.

Recent work (Xu et al., 2020; Agarwal et al., 2022) quantitatively evaluated the impacts of GC algorithms in a layer-wise fashion. They observe that GC can incur non-negligible compression overheads, but they have no solution to address the challenges of applying GC to DDT. HiPress (Bai et al., 2021) proposes a selective compression mechanism to determine whether to compress a tensor, but it still applies GC algorithms to a DDT job in a layer-wise fashion and incurs costly compression overheads. `Cupcake` uses a fusion fashion to minimize the incurred compression overheads.

Distributed deep learning frameworks batch multiple tensors for one communication operation to improve communication efficiency (Sergeev & Del Balso, 2018; Li et al., 2020; Chen et al., 2015; Romero et al., 2022). However, this mechanism takes place after compression and is orthogonal to GC algorithms. PipeSwitch (Bai et al., 2020) fuses tensors to pipeline model transmission over the PCIe for fast context switching of deep learning applications. In contrast, `Cupcake` fuses tensors to improve compression efficiency.

7 Conclusion

`Cupcake` is a general compression optimizer to enable GC algorithms to fully unleash their benefits to accelerate the training throughput of DDT jobs. Instead of compressing tensors in a layer-wise fashion, `Cupcake` applies GC algorithms in a fusion fashion and can find the provably optimal fusion strategy to maximize the training throughput of compression-enabled DDT. `Cupcake` can significantly improve the performance of DDT over full synchronization and solutions with layer-wise compression.

Acknowledgment

We would like to thank our shepherd Ang Li and the anonymous reviewers for providing valuable feedback. Zhuang Wang, Xinyu Crystal Wu, and T. S. Eugene Ng are partially supported by the NSF under CNS-2214272 and CNS-1815525.

References

Tensorflow: A system for large-scale machine learning. In *USENIX Symposium on Operating Systems Design and Implementation (OSDI)*, pp. 265–283, 2016.

NVIDIA NCCL. `https://developer.nvidia.com/NCCL`, 2021.

Agarwal, S., Wang, H., Venkataraman, S., and Papailiopoulos, D. On the utility of gradient compression in distributed training systems. *Proceedings of Machine Learning and Systems*, 4:652–672, 2022.

Aji, A. F. and Heafield, K. Sparse communication for distributed gradient descent. 2017.

Alistarh, D., Grubic, D., Li, J., Tomioka, R., and Vojnovic, M. QSGD: Communication-efficient SGD via gradient quantization and encoding. In *Advances in Neural Information Processing Systems*, pp. 1709–1720, 2017.

Arafa, Y., Badawy, A.-H. A., Chennupati, G., Santhi, N., and Eidenbenz, S. Low overhead instruction latency characterization for nvidia gpgpus. In *2019 IEEE High Performance Extreme Computing Conference (HPEC)*, pp. 1–8. IEEE, 2019.

Bai, Y., Li, C., Zhou, Q., Yi, J., Gong, P., Yan, F., Chen, R., and Xu, Y. Gradient compression supercharged high-performance data parallel dnn training. In *Proceedings of the ACM SIGOPS 28th Symposium on Operating Systems Principles*, pp. 359–375, 2021.

Bai, Z., Zhang, Z., Zhu, Y., and Jin, X. {PipeSwitch}: Fast pipelined context switching for deep learning applications. In *14th USENIX Symposium on Operating Systems Design and Implementation (OSDI 20)*, pp. 499–514, 2020.

Ben-Nun, T. and Hoefler, T. Demystifying parallel and distributed deep learning: An in-depth concurrency analysis. *ACM Computing Surveys (CSUR)*, 52(4):1–43, 2019.

Bernstein, J., Wang, Y.-X., Azizzadenesheli, K., and Anandkumar, A. signSGD: Compressed optimisation for non-convex problems. *arXiv preprint arXiv:1802.04434*, 2018.

ByteDance. BytePS. `https://github.com/bytedance/byteps`, 2020.

Chen, J., Pan, X., Monga, R., Bengio, S., and Jozefowicz, R. Revisiting distributed synchronous sgd. *arXiv preprint arXiv:1604.00981*, 2016.

Chen, T., Li, M., Li, Y., Lin, M., Wang, N., Wang, M., Xiao, T., Xu, B., Zhang, C., and Zhang, Z. Mxnet: A flexible and efficient machine learning library for heterogeneous distributed systems. *arXiv preprint arXiv:1512.01274*, 2015.

Chen, T., Moreau, T., Jiang, Z., Zheng, L., Yan, E., Shen, H., Cowan, M., Wang, L., Hu, Y., Ceze, L., et al. {TVM}: An automated end-to-end optimizing compiler for deep learning. In *13th {USENIX} Symposium on Operating Systems Design and Implementation ({OSDI} 18)*, pp. 578–594, 2018.

Deng, J., Dong, W., Socher, R., Li, L.-J., Li, K., and Fei-Fei, L. Imagenet: A large-scale hierarchical image database. In *2009 IEEE conference on computer vision and pattern recognition*, pp. 248–255. Ieee, 2009.

Dettmers, T. 8-bit approximations for parallelism in deep learning. *arXiv preprint arXiv:1511.04561*, 2015.

Devlin, J., Chang, M.-W., Lee, K., and Toutanova, K. Bert: Pre-training of deep bidirectional transformers for language understanding. *arXiv preprint arXiv:1810.04805*, 2018.

Fei, J., Ho, C.-Y., Sahu, A. N., Canini, M., and Sapio, A. Efficient sparse collective communication and its application to accelerate distributed deep learning. In *Proceedings of the 2021 ACM SIGCOMM 2021 Conference*, pp. 676–691, 2021.

Gupta, V., Choudhary, D., Tang, P. T. P., Wei, X., Wang, X., Huang, Y., Kejariwal, A., Ramchandran, K., and Mahoney, M. W. Fast distributed training of deep neural networks: Dynamic communication thresholding for model and data parallelism, 2020.

He, K., Zhang, X., Ren, S., and Sun, J. Deep residual learning for image recognition. In *Proceedings of the IEEE conference on computer vision and pattern recognition*, pp. 770–778, 2016.

Huang, Y., Cheng, Y., Bapna, A., Firat, O., Chen, D., Chen, M., Lee, H., Ngiam, J., Le, Q. V., Wu, Y., et al. Gpipe: Efficient training of giant neural networks using pipeline parallelism. *Advances in neural information processing systems*, 32:103–112, 2019.

Jiang, P. and Agrawal, G. A linear speedup analysis of distributed deep learning with sparse and quantized communication. In *Advances in Neural Information Processing Systems*, pp. 2525–2536, 2018.

Jiang, Y., Zhu, Y., Lan, C., Yi, B., Cui, Y., and Guo, C. A unified architecture for accelerating distributed {DNN} training in heterogeneous gpu/cpu clusters. In *14th {USENIX} Symposium on Operating Systems Design and Implementation ({OSDI} 20)*, pp. 463–479, 2020.

Karimireddy, S. P., Rebjock, Q., Stich, S. U., and Jaggi, M. Error feedback fixes signsgd and other gradient compression schemes. *arXiv preprint arXiv:1901.09847*, 2019.

Kingma, D. P. and Ba, J. Adam: A method for stochastic optimization. *arXiv preprint arXiv:1412.6980*, 2014.

Kiros, R., Zhu, Y., Salakhutdinov, R. R., Zemel, R., Urtasun, R., Torralba, A., and Fidler, S. Skip-thought vectors. In *Advances in neural information processing systems*, pp. 3294–3302, 2015.

Krizhevsky, A., Hinton, G., et al. Learning multiple layers of features from tiny images. 2009.

LeCun, Y., Bengio, Y., and Hinton, G. Deep learning. *nature*, 521(7553):436–444, 2015.

Li, M., Andersen, D. G., Park, J. W., Smola, A. J., Ahmed, A., Josifovski, V., Long, J., Shekita, E. J., and Su, B.-Y. Scaling distributed machine learning with the parameter server. In *USENIX Symposium on Operating Systems Design and Implementation (OSDI)*, 2014.

Li, S., Zhao, Y., Varma, R., Salpekar, O., Noordhuis, P., Li, T., Paszke, A., Smith, J., Vaughan, B., Damania, P., and Chintala, S. Pytorch distributed: Experiences on accelerating data parallel training. *arXiv preprint arXiv:2006.15704*, 2020.

Li, Y., Park, J., Alian, M., Yuan, Y., Qu, Z., Pan, P., Wang, R., Schwing, A., Esmaeilzadeh, H., and Kim, N. S. A network-centric hardware/algorithm co-design to accelerate distributed training of deep neural networks. In *2018 51st Annual IEEE/ACM International Symposium on Microarchitecture (MICRO)*, pp. 175–188. IEEE, 2018.

Lin, Y., Han, S., Mao, H., Wang, Y., and Dally, W. J. Deep gradient compression: Reducing the communication bandwidth for distributed training. *The International Conference on Learning Representations (ICLR)*, 2017.

Luo, L., Nelson, J., Ceze, L., Phanishayee, A., and Krishnamurthy, A. Parameter hub: a rack-scale parameter server for distributed deep neural network training. In *Proceedings of the ACM Symposium on Cloud Computing*, pp. 41–54, 2018.

Manning, C. D., Surdeanu, M., Bauer, J., Finkel, J. R., Bethard, S., and McClosky, D. The stanford corenlp natural language processing toolkit. In *Proceedings of 52nd annual meeting of the association for computational linguistics: system demonstrations*, pp. 55–60, 2014.

Mellanox. Mellanox Corporate Update. `https://www.mellanox.com/related-docs/company/MLNX_Corporate_Deck.pdf`, 2022.

NVIDIA. A Timeline of Innovation for NVIDIA. `ttps://www.nvidia.com/en-us/about-nvidia/corporate-timeline/`, 2021.

Owens, J. D., Houston, M., Luebke, D., Green, S., Stone, J. E., and Phillips, J. C. Gpu computing. *Proceedings of the IEEE*, 96(5):879–899, 2008.

Paszke, A., Gross, S., Massa, F., Lerer, A., Bradbury, J., Chanan, G., Killeen, T., Lin, Z., Gimelshein, N., Antiga, L., Desmaison, A., Kopf, A., Yang, E., DeVito, Z., Raison, M., Tejani, A., Chilamkurthy, S., Steiner, B., Fang, L., Bai, J., and Chintala, S. Pytorch: An imperative style, high-performance deep learning library. In *Advances in Neural Information Processing Systems*, pp. 8024–8035, 2019.

Rajpurkar, P., Jia, R., and Liang, P. Know what you don't know: Unanswerable questions for squad. *arXiv preprint arXiv:1806.03822*, 2018.

Renggli, C., Ashkboos, S., Aghagolzadeh, M., Alistarh, D., and Hoefler, T. Sparcml: High-performance sparse communication for machine learning. In *Proceedings of the International Conference for High Performance Computing, Networking, Storage and Analysis*, pp. 1–15, 2019.

Romero, J., Yin, J., Laanait, N., Xie, B., Young, M. T., Treichler, S., Starchenko, V., Borisevich, A., Sergeev, A., and Matheson, M. Accelerating collective communication in data parallel training across deep learning frameworks. In *19th USENIX Symposium on Networked Systems Design and Implementation (NSDI 22)*, pp. 1027–1040, 2022.

Sapio, A., Canini, M., Ho, C.-Y., Nelson, J., Kalnis, P., Kim, C., Krishnamurthy, A., Moshref, M., Ports, D. R., and Richtárik, P. Scaling distributed machine learning with in-network aggregation. *arXiv preprint arXiv:1903.06701*, 2019.

Seide, F., Fu, H., Droppo, J., Li, G., and Yu, D. 1-bit stochastic gradient descent and its application to data-parallel distributed training of speech dnns. In *Fifteenth Annual Conference of the International Speech Communication Association*, 2014.

Sergeev, A. and Del Balso, M. Horovod: fast and easy distributed deep learning in tensorflow. *arXiv preprint arXiv:1802.05799*, 2018.

Shallue, C. J., Lee, J., Antognini, J., Sohl-Dickstein, J., Frostig, R., and Dahl, G. E. Measuring the effects of data parallelism on neural network training. *Journal of Machine Learning Research*, 20:1–49, 2019.

Shi, S., Zhou, X., Song, S., Wang, X., Zhu, Z., Huang, X., Jiang, X., Zhou, F., Guo, Z., Xie, L., et al. Towards scalable distributed training of deep learning on public cloud clusters. *Proceedings of Machine Learning and Systems*, 3:401–412, 2021.

Simonyan, K. and Zisserman, A. Very deep convolutional networks for large-scale image recognition. *arXiv preprint arXiv:1409.1556*, 2014.

Stich, S. U., Cordonnier, J.-B., and Jaggi, M. Sparsified SGD with memory. In *Advances in Neural Information Processing Systems*, 2018.

Strom, N. Scalable distributed dnn training using commodity gpu cloud computing. In *Sixteenth Annual Conference of the International Speech Communication Association*, 2015.

Sun, P., Feng, W., Han, R., Yan, S., and Wen, Y. Optimizing network performance for distributed dnn training on gpu clusters: Imagenet/alexnet training in 1.5 minutes. *arXiv preprint arXiv:1902.06855*, 2019.

Szegedy, C., Vanhoucke, V., Ioffe, S., Shlens, J., and Wojna, Z. Rethinking the inception architecture for computer vision. In *Proceedings of the IEEE conference on computer vision and pattern recognition*, pp. 2818–2826, 2016.

Thakur, R., Rabenseifner, R., and Gropp, W. Optimization of collective communication operations in MPICH. *The International Journal of High Performance Computing Applications*, 19(1), 2005.

Tsuzuku, Y., Imachi, H., and Akiba, T. Variance-based gradient compression for efficient distributed deep learning. *arXiv preprint arXiv:1802.06058*, 2018.

Vogels, T., Karimireddy, S. P., and Jaggi, M. Powersgd: Practical low-rank gradient compression for distributed optimization. *arXiv preprint arXiv:1905.13727*, 2019.

Wang, H., Sievert, S., Charles, Z., Liu, S., Wright, S., and Papailiopoulos, D. Atomo: Communication-efficient learning via atomic sparsification. *arXiv preprint arXiv:1806.04090*, 2018a.

Wang, H., Sievert, S., Liu, S., Charles, Z., Papailiopoulos, D., and Wright, S. Atomo: Communication-efficient learning via atomic sparsification. *Advances in Neural Information Processing Systems*, 31, 2018b.

Wang, L., Wu, W., Zhang, J., Liu, H., Bosilca, G., Herlihy, M., and Fonseca, R. Fft-based gradient sparsification for the distributed training of deep neural networks. In *Proceedings of the 29th International Symposium on High-Performance Parallel and Distributed Computing*, pp. 113–124, 2020.

Wang, Z., Xu, Z., Wu, X., Shrivastava, A., and Ng, T. E. Dragonn: Distributed randomized approximate gradients of neural networks. In *International Conference on Machine Learning*, pp. 23274–23291. PMLR, 2022.

Wang, Z., Lin, H., Zhu, Y., and Ng, T. E. Hi-speed dnn training with espresso: Unleashing the full potential of gradient compression with near-optimal usage strategies. In *Proceedings of the Eighteenth EuroSys Conference*, 2023.

Wen, W., Xu, C., Yan, F., Wu, C., Wang, Y., Chen, Y., and Li, H. Terngrad: Ternary gradients to reduce communication in distributed deep learning. In *Advances in neural information processing systems*, pp. 1509–1519, 2017.

Wu, J., Huang, W., Huang, J., and Zhang, T. Error compensated quantized SGD and its applications to large-scale distributed optimization. *arXiv preprint arXiv:1806.08054*, 2018.

Xu, H., Ho, C.-Y., Abdelmoniem, A. M., Dutta, A., Bergou, E. H., Karatsenidis, K., Canini, M., and Kalnis, P. Compressed communication for distributed deep learning: Survey and quantitative evaluation. Technical report, 2020.

Zhang, H., Zheng, Z., Xu, S., Dai, W., Ho, Q., Liang, X., Hu, Z., Wei, J., Xie, P., and Xing, E. P. Poseidon: An efficient communication architecture for distributed deep learning on GPU clusters. In *2017 USENIX Annual Technical Conference (ATC)*, pp. 181–193, 2017.

Zhang, Z., Chang, C., Lin, H., Wang, Y., Arora, R., and Jin, X. Is network the bottleneck of distributed training? In *Proceedings of the Workshop on Network Meets AI & ML*, pp. 8–13, 2020.

Zheng, L., Jia, C., Sun, M., Wu, Z., Yu, C. H., Haj-Ali, A., Wang, Y., Yang, J., Zhuo, D., Sen, K., et al. Ansor: Generating high-performance tensor programs for deep learning. In *14th {USENIX} Symposium on Operating Systems Design and Implementation ({OSDI} 20)*, pp. 863–879, 2020.

Zinkevich, M., Weimer, M., Smola, A. J., and Li, L. Parallelized stochastic gradient descent. In *NIPS*, volume 4, pp. 4. Citeseer, 2010.